Michigan State University

National Superconducting Cyclotron Laboratory

CORRELATIONS IN NUCLEAR ARRHENIUS-TYPE PLOTS

M.B. TSANG and P. DANIELEWICZ

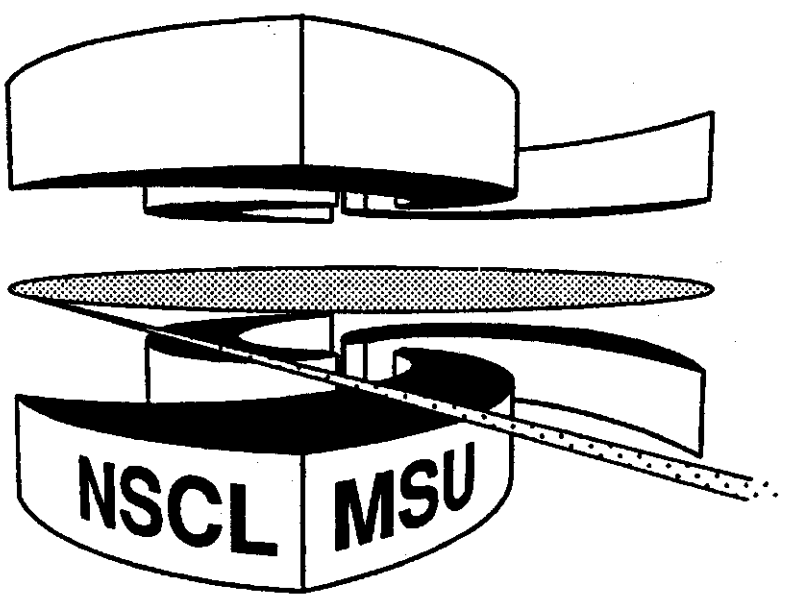

MSUCL-1069

APRIL 1997

Correlations in Nuclear Arrhenius-Type Plots

M. B. Tsang and P. Danielewicz

National Superconducting Cyclotron Laboratory and Department of Physics and Astronomy,

Michigan State University, East Lansing, MI 48824, USA,

(April 25, 1997)

Abstract

Arrhenius-type plots for multifragmentation process, defined as the transverse energy dependence of the single-fragment emission-probability, ($\ln(1/p_b)$ vs $1/\sqrt{E_t}$), have been studied by examining the relationship of the parameters p_b and E_t to the intermediate-mass fragment multiplicity $\langle n \rangle$. The linearity of these plots reflects the correlation of the fragment multiplicity with the transverse energy. These plots may not provide thermal scaling information about fragment production as previously suggested.

About a hundred years ago, the Swedish chemist Svante Arrhenius discovered that the rate of chemical reactions increases with temperature [1]. Specifically, the chemical reaction rate constant (k) is related to the absolute temperature (T) by

$$k \propto \exp(-E_a/T) \tag{1}$$

where E_a is the activation energy of the chemical reaction. The linear relationship between $\ln(k)$ and $1/T$ is widely known as Arrhenius plot in chemistry and is associated with thermal equilibrium processes.

Recently, Arrhenius-type plots have been used to study the statistical [2-5] and dynamical [6] properties of fragment emissions in heavy ion reactions. In the intermediate incident energy range, between few tens of MeV to 100 MeV per nucleon, the production of intermediate mass fragments (IMF, $3 \leq Z \leq 20$), also known as multifragmentation, is an important decay mode of highly excited nuclear systems [7]. Calculations suggest that the fragments are produced in the phase co-existence region. Thus, understanding the mechanisms of fragment formation may provide an insight to the liquid gas phase transition in nuclear matter [7].

Several experiments [2-4] gave evidence that in collisions characterized by a given value of the total transverse energy of detected charged particles,

$$E_t = \sum_i E_i \sin^2 \theta_i, \tag{2}$$

the IMF multiplicity distribution may be fitted by a binomial distribution,

$$P_n^m = \frac{m!}{n!(m-n)!} p_b^n (1-p_b)^{m-n}, \tag{3}$$

where n is the IMF multiplicity and the parameter m is interpreted as the number of times the system tries to emit a fragment. The probability of emitting fragments can be reduced to a single particle emission probability p_b for true binomial distributions; the binomial parameters m and p_b are related to the mean and variance of the fragment multiplicity distributions according to:

$$\langle n \rangle = m p_b \tag{4}$$

$$\sigma_n^2 = \langle n \rangle (1 - p_b) \tag{5}$$

The past investigations found a simple linear relationship between $\ln(1/p_b)$ and $1/\sqrt{E_t}$ (nuclear Arrhenius-type plots), for several projectile-target combinations and incident energies [2-4]. By assuming a linear relationship between $\sqrt{E_t}$ and temperature T and from the linearity of the observed $\ln(1/p_b)$ vs $1/\sqrt{E_t}$ plot, it has been inferred that a thermal scaling of the multifragment processes might be a general property [2-4]. In this picture, the observed "linear" dependence of $\ln(1/p)$ upon $1/T$ would be reflecting the

$$p \propto \exp(-B/T) \tag{6}$$

dependence of fragment emission probabilities upon a common fragment emission barrier B.

However, unlike chemical reactions, p and T were not measured directly in Refs. [2-4]. There, the validity of the Arrhenius-type plots relies on two assumptions: 1) that E_t is proportional to the excitation energy E^*, and therefore, should be proportional to T^2, and 2) that p_b obtained by fitting the fragment multiplicity distributions is the elementary emission probability p. This article will examine the above assumptions and investigate the underlying reasons for the linearity exhibited by the Arrhenius-type plots obtained in many systems.

The assumption that temperature is proportional to the square root of the excitation energy, $T \propto \sqrt{E^*}$, is valid for compound nuclei formed at low to moderate temperature. Some relationship between the transverse energy and excitation energy and therefore temperature may also be obtained for compound nuclei, provided adjustment is made for the Coulomb barrier and for neutron emission [8]. For the intermediate-energy heavy ion reactions such as $^{36}Ar + ^{197}Au$ at $E/A = 35$ to 110 MeV, where linearity of the Arrhenius-type plots have been observed, however, the final states contain fast particles emitted from the overlap region of projectile and target as well as delayed emission from projectile- and target-like residues. In particular, particle production from the overlap participant region dominates

in central collisions [9-12], and the transverse energy from this region is strongly affected by the collective motion [13]. There has never been any unambiguous experimental evidence supporting that $\sqrt{E_t}$ is proportional to the temperature and in fact the evidence is to the contrary. Recent temperature measurements using both the excited states populations and isotope yield ratios show that the temperature dependence on the impact parameter determined from charge particle multiplicities is very weak [14-16], less than 1 MeV from peripheral to central collisions. Similar trends have also been observed for the $Ar + Au$ reactions at $E/A = 35MeV$ [17]. Since E_t is strongly impact parameter dependent [18], these temperature measurements thus imply that E_t is independent of temperature and the assumption that $T \propto \sqrt{E_t}$ is not valid. Based on this argument alone, the $\ln(1/p_b)$ vs $1/\sqrt{E_t}$ plot is not the Arrhenius plot analogous to that observed in chemical reactions. The breakdown of the $T \propto \sqrt{E_t}$ assumption suggests that previous interpretation of thermal scaling on emission probabilities, charge distributions and azimuthal correlations [2-4, 20-23] should be re-examined.

Next, we will examine the assumptions used to extract the fragment emission probability. There is no apriori reason for the emitted fragments to prefer binomial statistics or Poissonian statistics. In Poissonian statistics, the probability of emitting n fragments is

$$P_p(n) = \frac{\lambda^n}{n!}e^{-\lambda} \tag{7}$$

where $\lambda = \langle n \rangle$ is the mean. The major difference between the binomial and Poisson distributions is the ratio of the variance to the mean, $\sigma^2/\langle n \rangle$ where $\sigma^2/\langle n \rangle = 1$ for Poisson distribution and < 1 for binomial distribution. It has been demonstrated that constraints from conservation laws reduce the width of the Poisson distributions to much less than 1 [19]. For example, if charge conservation constraint is applied to a Poissonian distribution, Eq. (7) is modified to (see Appendix)

$$P_m(n, \alpha) = \frac{\lambda^n}{n!}e^{-\lambda}e^{-\alpha(n-\lambda)^2} \tag{8}$$

where α is the charge constraint factor.

For small α, the mean fragment multiplicity for Eqs. (7) and (8) are nearly the same; $\langle n \rangle \approx \lambda$. Fig. 1 shows three modified Poisson distributions of Eq. (8) (solid and open points) for $\lambda = 3$, 6 and 10 and $\alpha = 0.1$. To illustrate that distributions such as Eq. (8) whose values of $\sigma^2/\langle n \rangle$ are less than 1 can be described by binomial distributions, we used Eqs. (4) and (5) to determine the binomial parameters m and p_b whose values are listed in Fig. 1. The solid and dashed lines are binomial distributions of Eq. (3). The agreement between the two distributions is very good. However, in this context, m and p_b are mainly fit parameters used to describe the modified Poisson distributions of Eq. (8) and p_b is not an elementary emission probability. If the small values of $\sigma^2/\langle n \rangle$ reflect the constraints of conservation laws of Eq. (8) observed in Ref. [19], the reducibility of fragments emission to binomial distributions shown by Refs. [2-4] does not imply any fundamental significance for the parameters m and p_b thereby extracted.

Even though the $\ln(1/p_b)$ vs $1/\sqrt{E_t}$ plots constructed in heavy ion reactions are not true Arrhenius plots, analyses of many systems [2-4, 25] suggest that the approximate linearity of such plots may be universal. To explain this appealing systematics, we examine the correlations between the observable E_t, parameter p_b, and the fragment multiplicity n [25]. Since E_t is obtained from the measured energies of both the light particles and fragments, Eq. (2), the energy and multiplicities are related by

$$E_t \approx (N_C - \langle n \rangle) E_t^{LP} + \langle n \rangle E_t^{IMF}, \quad (9)$$

where N_C is the total charge particle multiplicities, E_t^{LP} and E_t^{IMF} are the average transverse energy of a light particle and an IMF, respectively. Experimentally, the dependence of N_C on $\langle n \rangle$ can be approximated by [9-12]

$$N_C = a' + b' \langle n \rangle \quad (10)$$

where a' corresponds to the typical number of light charge particles emitted before any IMF is emitted and b' is the number of light charge particle emitted for each IMF emitted. There is some non-linear dependence of $\langle n \rangle$ at very high N_C, where $\langle n \rangle$ saturates for central

collision, and at very low N_C, where fluctuations in small value of n prevent a sharp cutoff in N_c. Except for very large and small values of N_c, Eq. (9) can be then rewritten into:

$$E_t = a + b\langle n\rangle = b(a/b + \langle n\rangle) \tag{11}$$

where $a = a' E_t^{LP}$ is the threshold transverse energy associated with light particles emitted before any IMF and $b = (b' - 1)E_t^{LP} + E_t^{IMF}$.

The binomial fit parameter m is nearly constant as a function of the transverse energy E_t [2-4]. Thus the plots of $\ln(1/p_b)$ vs $1/\sqrt{E_t}$ can now be reduced to $\ln(1/\langle n\rangle)$[26] vs $1/\sqrt{a/b + \langle n\rangle}$ according to Eqs. (4) and (11). Fig. 2 shows the dependence of $1/\langle n\rangle$ and $1/\sqrt{a/b + \langle n\rangle}$ for $\langle n\rangle$ ranging from 0.25 to 5.0, typical values observed in multifragmentation of heavy ion reactions [2-4,9-12]. For $a/b = 0$, the curve is concave and for $a/b = 1$, the curve becomes slightly convex. In the middle region, where $a/b \approx 0.5$, the curve is nearly linear. Thus the linearity of the Arrhenius-type plots merely reflects the correlation of the fragment multiplicity with itself when the value of a/b is about 0.5 which naturally arises from the intrinsic linear dependence of $\langle n\rangle$ on E_t.

To illustrate the self-correlation effect in nuclear Arrhenius-type plots, the published data for the $Ar + Au$ collisions at $E/A = 110$ MeV [2, 4] are plotted as solid points in the left panel of Fig. 3. The solid line is the self-correlation of $1/\langle n\rangle$ and $1/\sqrt{a/b + \langle n\rangle}$, scaled according to Eqs. (4) and (11) using the experimental determined values of $m = 12$ [2, 4], $a/b = 0.5$, $b = 213$ MeV [2, 4, 24]. The good agreement between the data and the self correlation confirms that the linearity observed in the Arrhenius-type plot mainly comes from the linear dependence of E_t on $\langle n\rangle$ with a non-zero offset in Eq. (11).

The non-zero value of a arises from Eq. (10) because a' is not zero. One would expect that a relation between $1/\langle n\rangle$ and $1/\sqrt{N_c}$ similar to those shown in Fig. 2 should be observed. The right panel of Figure 3 shows the plot of $1/\langle n\rangle$ vs $1/\sqrt{N_c}$ for $Ar + Au$ reaction at $E/A = 110$ MeV [2,4,24]. The linearity is of the plot is comparable to most Arrhenius-type plots [2-4, 25]. Since $\langle n\rangle$ and N_C are much less affected by the energy resolution of the detection device, they are better observables than p_b and E_t used in the Arrhenius-

type plots. Figure 3 suggests that the Arrhenius-type plots contain essentially the same information as the much simpler plots of the IMF multiplicity ($\langle n \rangle$) as a function of charge particle multiplicity (N_C) published in many studies [9-12].

In summary, recent temperature measurements show that temperature is nearly independent of impact parameter and therefore the transverse energy E_t is not related to temperature. If $\sqrt{E_t}$ is not proportional to the temperature, $\ln(1/p_b)$ vs $1/\sqrt{E_t}$ are not true Arrhenius plots. Without invoking the interpretation of fragment emission probability in binomial distributions or the temperature dependence of E_t, the linearity of the Arrhenius-type plots can be reproduced from the linear dependence of E_t on fragment multiplicity $\langle n \rangle$. These plots carry the same information as N_C vs $\langle n \rangle$ plots and do not provide additional information concerning the thermal scaling of fragment emissions.

Appendix

When many independent processes contribute to the multiplicity of certain particles, each with a small probability, then the multiplicity is expected to obey a Poisson distribution. Within the grand canonical ensemble, a Poisson distribution also follows. In general, the Poisson distribution is associated with a large overall system compared to the subsystem studied. However, in heavy ion reactions, the systems studied are always finite, constrained by conservation laws such as the overall energy, charge, and mass conservation within the participant region.

To investigate the minimal effect of the above mentioned constraints on the multiplicity distribution of IMF, we first consider a situation where probabilities of emitting various individual particles are independent, with multiplicities being governed by a Poisson distribution in the absence of any constraint. When multiplicities of individual IMFs are governed by a Poisson distribution, then the overall multiplicity of IMFs is also governed by a Poisson distribution [27]. For simplicity, we next impose only a single constraint, that of the charge conservation, and examine changes in the multiplicity distribution of IMF. The constraint modifies the Poisson distribution to

$$P_m(n) \propto \sum_{\{n_\nu:\nu\in\mathrm{IMF}\}} \delta_{n,\sum_\mu n_\mu} \prod_\tau \left(P_p^\tau(n_\tau)\right) \sum_{Z_{oth}} \mathcal{P}_{oth}(Z_{oth})\, \delta_{Z,Z_{oth}+\sum_\rho n_\rho z_\rho}. \tag{12}$$

where P_p^τ is a Poisson distribution for fragment τ, $\mathcal{P}_{oth}$ is the charge distribution of all particles other than IMF, and Z is the charge of the emitting source, $Z = \langle Z_{oth}\rangle + \sum_\nu \langle n_\nu\rangle z_\nu$. If the system emits a lot more other particles than IMF, from the central-limit theorem, $\mathcal{P}_{oth}$ is expected to be close to a Gaussian function,

$$\mathcal{P}_{oth}(Z_{oth}) \propto \exp\left(-\frac{(Z_{oth}-\langle Z_{oth}\rangle)^2}{2\,\sigma^2(Z_{oth})}\right). \tag{13}$$

The dispersion in Eq. (13) should be primarily associated with light (Z=1 and Z=2) particles in the participant region, and, possibly, to some extent with the amount of charge that the spectator matter carries off. From the central-limit theorem, given Poisson distributions, the dispersion is then $\sigma^2(Z_{oth}) \gtrsim \langle n_{Z=1}\rangle + 4\langle n_{Z=2}\rangle$. Substituting Eq. (13) into Eq. (12) we get

$$P_m(n) \propto \sum_{\{n_\nu:\nu\in\mathrm{IMF}\}} \delta_{n,\sum_\mu n_\mu} \prod_\tau \left(P_p^\tau(n_\tau)\right) \exp\left(-\frac{\left(\sum_\nu (n_\nu-\langle n_\nu\rangle) z_\nu\right)^2}{2\,\sigma^2(Z_{oth})}\right). \tag{14}$$

Finally, to assess the effect of the constraining factor in Eq. (14) we approximate the charge in the exponential by its average value, $z_\nu \approx \langle z\rangle = \sum_\mu \langle n_\mu\rangle z_\mu / \langle n\rangle$, and obtain

$$P_m(n) \propto P_p(n) \exp\left(-\alpha(n-\langle n\rangle)^2\right), \tag{15}$$

where $\alpha = \langle z\rangle^2/2\,\sigma^2(Z_{oth}) \lesssim \langle z\rangle^2/2(\langle n_{Z=1}\rangle + 4\langle n_{Z=2}\rangle)$. Charged particle multiplicities measured in Ref. [24] suggest $\alpha \lesssim 0.2$.

The main effect of the constraint in Eq. (15) is to narrow the multiplicity distribution, compared to the Poisson distribution. Depending on correlations between charge, mass, and energy within the rest of the system, the other constraints may affect the multiplicity distributions further.

This work is supported by the National Science Foundation under Grant numbers PHY-95-28844 and PHY-9403666.

REFERENCES

[1] S. Arrhenius, Z. Phys. Chem., **4**, 226 (1889).

[2] L. G. Moretto et al., Phys. Rev. Lett. **74**, 1530 (1995).

[3] K. Tso et al., Phys. Lett. **B 361**, 25 (1995).

[4] L. G. Moretto, R. Getti, L. Phair, K. Tso and G. J. Wozniak, LBL 39388 (1996), submitted to Phys. Rep.

[5] A.S. Botvina, D.H.E. Gross, Phys. Lett. **B**, 344, 6 (1995)

R. Donangelo and S. Souza, preprint of Universidade Federal Do Rio De Janeiro, **if/ufrj/96**.

[6] J. Toke, D. K. Agnihotri, B. Djerroud, W. Skulski, and W.U. Schroder, University of Rochester preprint, submitted to PRC Rapid Communications.

[7] W. G. Lynch, Ann Rev of Nucl & Part. Sci. **37**, 493 (1987) and references therein.

L. G. Moretto and G. J. Wozniak, Ann. Rev. of Nucl & Part Sci, **43**, 379 (1993).

D. H. E. Gross, Rep. Progr. Phys. **53**, 605 (1990).

[8] A. Chbihi et al., Phys. Rev. **C 43**, 652 (1991).

A. Chbihi et al., Phys. Rev. **C 43**, 666 (1991).

R. Wada et al., Phys. Rev. **C 39**, 497 (1989).

G. Nebbia et al., Phys. Lett. **B 176**, 20 (1986).

M. Gonin et al., Phys. Lett **B 217**, 406 (1989).

[9] D. R. Bowman et al, Phys. Rev. Lett. **70**, 3534 (1993)

G. Peaslee et al., Phys. Rev. **C 49**, R2271 (1994).

[10] L. Phair et al., Phys. Lett. **B 285**, 10 (1992).

[11] K. Kwiatkowski et al., Phys. Rev. Lett. **74**, 3756 (1995).

J.C. Steckmeyer et al., Proceedings of the XXXIII[rd] International Winter Meeting on Nuclear Physics, Bormio, Italy, edited by I. Iori (Universita di Milano, Milano, Italy, 1995).

[12] G.J. Kunde, Phys. Rev. Lett. **77**, 2897 (1996).

Dempsey et al, Phys. Rev. C **54**, 1710 (1996).

J. Toke et al., Phys. Rev. Lett. **77**, 3514 (1996).

[13] C. Williams et al., Phys. Rev. **C56**, in press.

R. deSouza, Phys. Lett. **B300**, 29 (1992).

[14] M. J. Huang et al., Phys. Rev. Lett. **77**, 1648 (1997)

[15] H. Xi et al., MSU preprint, MSUCL-1055, (1997).

[16] M.J. Huang, PhD Thesis, Michigan State University (1997).

[17] F. Zhu et al., Phys. Lett B. **282**, 299 (1992).

F. Zhu et al., Phys. Rev. C **52**, 784 (1992).

[18] L. Phair et al, Nucl. Phys. **A548**, 489 (1992).

[19] L. Phair et al., Phys. Lett. **B 291**, 7 (1992).

[20] L. Phair et al., Phys. Rev. Lett. **75**, 213 (1995).

[21] L.G. Moretto et al., Phys. Rev. Lett. **75**, 4186 (1995).

[22] A. Ferrero et al., Phys. Rev. C **53**, R5 (1996).

[23] L. Phair et al., Phys. Rev. Lett. **77**, 822 (1996).

[24] L. Phair et al., PhD Thesis, Michigan State University (1993)

[25] W. Skulski et al., proceedings of 13th Winter Workshop on Nuclear Dynamics, Marathon, Fl, Feb 2-7, (1997).

[26] The mean IMF multiplicity $\langle n \rangle = mp_b$ is relatively free of experimental and energy resolution distortions. These distortion effects affect p_b and m in the opposite way so that the effects cancel out for the product of mp_b[6].

[27] N.G. Van Kampen, Stochastic Processes in Physics and Chemistry, North-Holland, Amsterdam, 1981.

FIGURES

FIG. 1. Three probability distributions for the constrained Poisson distributions of Eq. (8), for $\alpha = 0.1$, $\lambda = 3$ (solid points), $\lambda = 6$ (open points) and $\lambda = 10$ (solid points). The solid and dashed lines are fits with the binomial distributions, Eqs. (3-5). The corresponding fitting parameters, m and p_b are listed in the figure.

FIG. 2. Dependence of $1/n$ on $1/\sqrt{a/b + \langle n \rangle}$ for a/b =0, 0.5 and 1.0.

FIG. 3. Left panel: Arrhenius-type plot for the $Ar + Au$ reaction at $E/A = 110$ MeV [2, 4]. The solid line is the self-correlation of $1/\langle n \rangle$ as a function of $1/\sqrt{0.5 + \langle n \rangle}$ scaled according to Eqs. (4) and (11). Right panel: Dependence of $1/\langle n \rangle$ on $1/\sqrt{N_c}$.

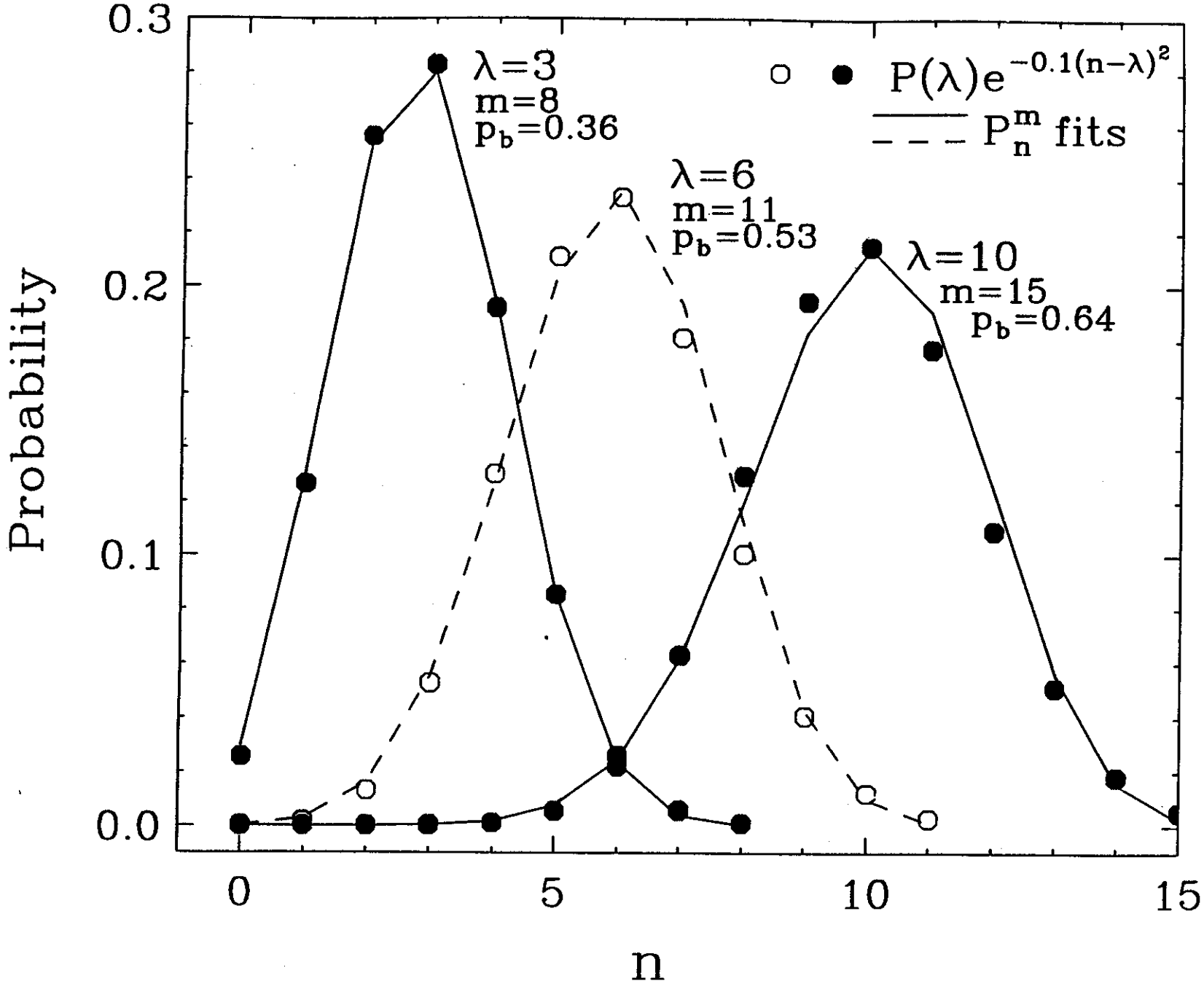
0.3
0.2
0.1
0.0
Probability
0
5
10
15
n
λ=3
m=8
p_b=0.36
λ=6
m=11
p_b=0.53
λ=10
m=15
p_b=0.64
P(λ)e^{-0.1(n-λ)^2}
P_n^m fits

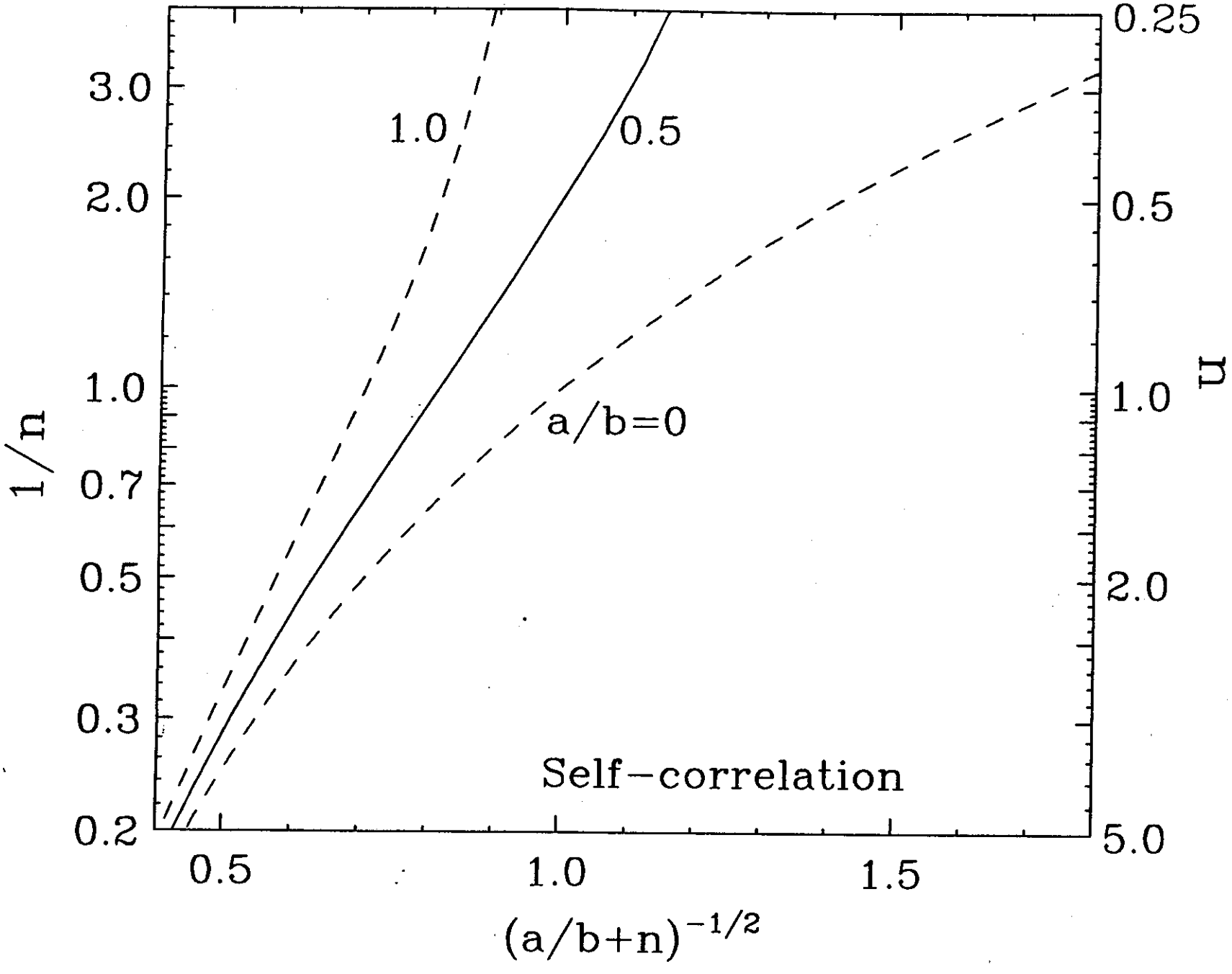
3.0
2.0
1.0
0.7
0.5
0.3
0.2
1/n
0.25
0.5
1.0
2.0
5.0
n
1.0
0.5
a/b=0
Self−correlation
0.5
1.0
1.5
(a/b+n)^-1/2

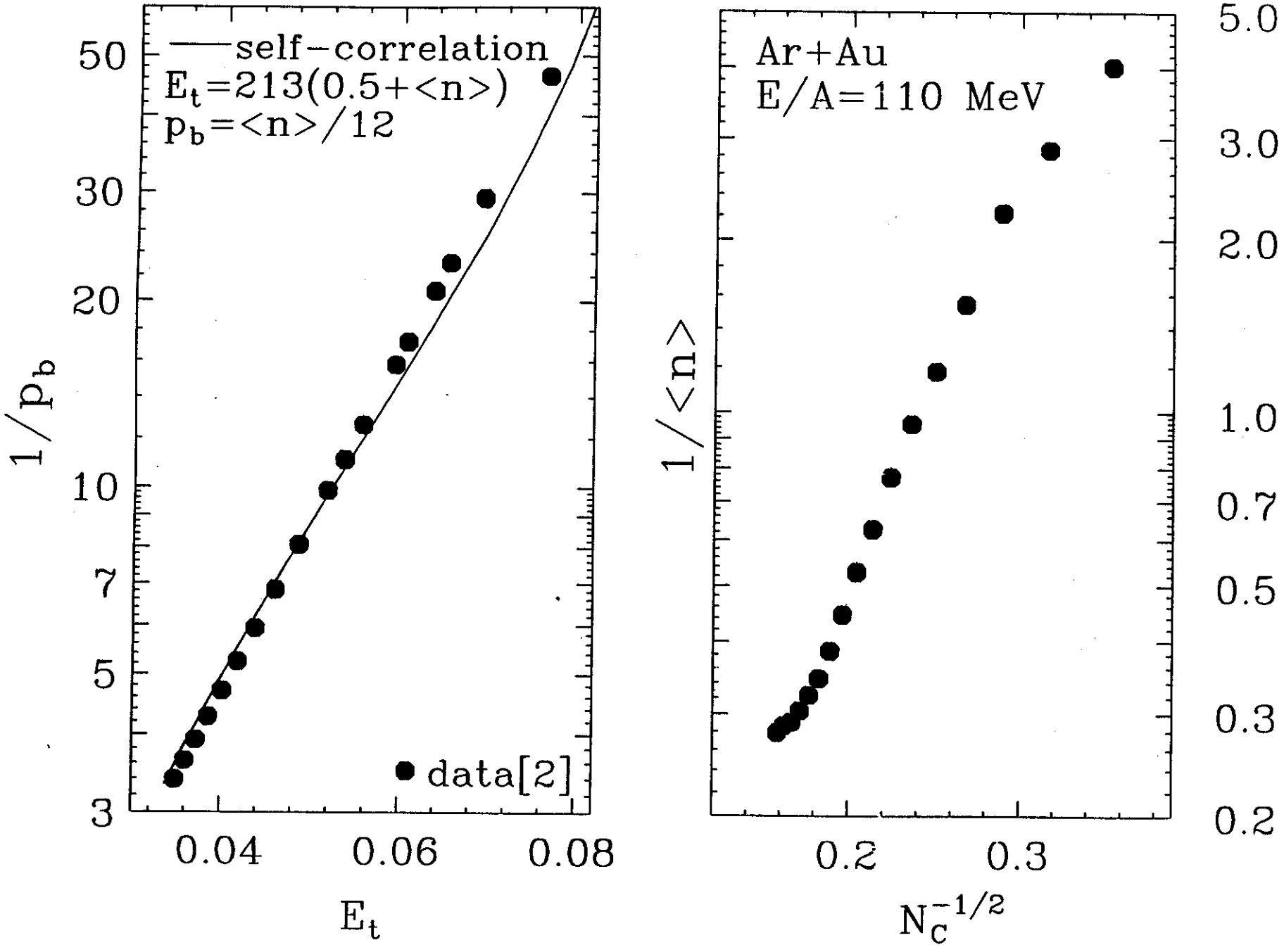
self−correlation
E_t=213(0.5+<n>)
p_b=<n>/12
data[2]
50
30
20
10
7
5
3
$1/p_b$
0.04
0.06
0.08
E_t
Ar+Au
E/A=110 MeV
5.0
3.0
2.0
1.0
0.7
0.5
0.3
0.2
$1/<n>$
0.2
0.3
$N_C^{-1/2}$